Scripta Materialia 185 (2020) 181–186

Contents lists available at ScienceDirect

Scripta Materialia

journal homepage: www.elsevier.com/locate/scriptamat

Realization of ultra-low thermal expansion over a broad temperature interval in $Gd_x(Dy_{0.5}Ho_{0.5})_{1-x}Co_2$ compounds

Jia-Zheng Hao[a,d,#], Fei-Ran Shen[a,b,f,#], Feng-Xia Hu[a,b,c,*], Hou-Bo Zhou[a,b], Zi-Bing Yu[a,b], Yi-Hong Gao[a,b], Wen-Hui Liang[a,b], Kai-Ming Qiao[a,b], Bing-Jie Wang[a,b], Jia Li[a,b], Cheng Zhang[a,b], Jing Wang[a,b,e], Lun-Hua He[a,c,f,*], Tian-Jiao Liang[f], Jun He[d], Ji-Rong Sun[a,b,c], Bao-Gen Shen[a,b,c,*]

[a] Beijing National Laboratory for Condensed Matter Physics & State Key Laboratory of Magnetism, Institute of Physics, Chinese Academy of Sciences, Beijing 100190, P. R. China
[b] School of Physical Sciences, University of Chinese Academy of Sciences, Beijing 100049, P. R. China
[c] Songshan Lake Materials Laboratory, Dongguan, Guangdong 523808, P. R. China
[d] Division of Functional Material Research, Central Iron and Steel Research Institute, Beijing 100081, P. R. China
[e] Fujian Innovation Academy, Chinese Academy of Sciences, Fuzhou, Fujian 350108, P. R. China
[f] China Spallation Neutron Source (CSNS), Dongguan 523808, China

ARTICLE INFO

Article history:
Received 4 March 2020
Revised 20 April 2020
Accepted 29 April 2020
Available online 20 May 2020

Keywords:
Zero thermal expansion (ZTE) materials
Magnetostriction
Phase transformation

ABSTRACT

Zero thermal expansion (ZTE) materials, particularly metals, have important applications in precision manufacturing. Here, ultra-low thermal expansion over a significantly broadened temperature interval is realized by tuning Gd content in ferrimagnetic(FIM) $Gd_x(Dy_{0.5}Ho_{0.5})_{1-x}Co_2$ compounds. The achieved coefficients of thermal expansion α_l ~+1.3 × $10^{-6}K^{-1}$ (5-220K), -1.5 × $10^{-6}K^{-1}$ (220-280K) for x=0.5 are even better than the well-known ZTE Invar alloy $Fe_{0.65}Ni_{0.35}$, while the operation temperature interval is much wider. The origin is closely related to the regulation of magnetostrictive process by rare earth ions along c-axis in the rhombohedral FIM structure. Our work highlights the advantageous ways to generate ultra-low thermal expansion in magnetocaloric materials.

Zero thermal expansion (ZTE) materials are widely used in precision manufacturing industry because of the advantages of invariable length with temperature. ZTE can be normally realized through combining positive thermal expansion (PTE) and negative thermal expansion (NTE) materials. However, from the perspective of practical application, a better way is to explore ZTE in a single material. Since the discovery of ZTE Invar alloys Fe-Ni [1], a lot of efforts have been made on anomalous thermal expansion and several categories of materials have been discovered showing useful NTE or ZTE, but most of them are nonmetallic materials. For example, the identified NTE materials include ZrW_2O_8 [2], CuO nanoparticles [3], $PbTiO_3$-based compounds [4], antiperovskite manganese nitrides [5-8], $La(Fe,Co,Si)_{13}$ [9], MnCoGe-based materials [10], reduced Ca_2RuO_4 [11] and etc.. While the ZTE materials include $Zr_{1-x}Sn_xMo_2O_8$ [12], tetramethylammonium copper(I) zinc(II) cyanide [13], β-eucryptite [14], ReO_3-based fluorides [15], $Fe[Co-(CN)_6]$ [16], Mn-based antiperovskites [8,17], and $Tb(Co,Fe)_2$. [18] Because of the advantages of high electrical/thermal conductivity of metals, exploring intermetallics with ZTE in a broadened temperature interval is still a challenge.

Magnetocaloric effect (MCE) has attracted much attention because of its useful applications in magnetic refrigeration technique [19-25]. A common feature of these materials is the magnetostructural/magnetoelastic transition involving strong spin-lattice coupling. The abnormal lattice expansion caused by magnetic interactions in the MCE materials provides a feasible platform for exploring NTE or ZTE.

The Laves phase intermetallic compounds RCo_2 (R: rare earth) are promising candidates for magnetic refrigerants owing to their large MCE [25-27]. In particular, $ErCo_2$ was recognized as the most representative MCE material in the low-temperature region with magnetic entropy change as high as -ΔS~37.2 J $kg^{-1}K^{-1}$for 0-5T around Curie temperature T_C ~32K [25]. The high magnetic moment contributed by R atoms and considerable lattice distortion around T_C were considered to be the origin of giant MCE. In RCo_2, the magnetic ordering of Co sublattices is not intrinsic but caused by rare earth molecular field [28,29]. For example, when the R

* Corresponding authors.
E-mail addresses: fxhu@iphy.ac.cn (F.-X. Hu), lhhe@iphy.ac.cn (L.-H. He), shenbg@iphy.ac.cn (B.-G. Shen).
# These two authors contribute equally to this work.

https://doi.org/10.1016/j.scriptamat.2020.04.043
1359-6462/

sites are filled by the non-magnetic Y and Lu ions, the exchange-enhanced Pauli paramagnetism prevails in the sample [28]. In contrast, Co moment can be induced by the exchange interactions between 4f and 3d spins when the rare earth elements occupy R sites. For heavy rare earth (Gd, Tb, Dy, Ho, Er), the exchange coupling between R and Co ions results in ferrimagnetic (FIM), while ferromagnetic (FM) behavior for light rare earth elements [29]. $ErCo_2$, $HoCo_2$ and $DyCo_2$ behave first-order transition and considerable magnetovolume effect, where an abnormal lattice contraction occurs during the magnetostructural transition from FIM to paramagnetic (PM) phase [25,30,31]. However, the first-order transition nature and lattice distortion become less significant with increasing the R element number. For $TbCo_2$ and $GdCo_2$, both theoretical and experimental studies demonstrated second-order type transition with neglectable lattice distortion around T_C [32,33]. Therefore, it is expected that the proper mixing of rare earth elements at R sites can adjust the magnetovolume effect to a large extent and achieve ultra-low thermal expansion.

We synthesized $Gd_x(Dy_{0.5}Ho_{0.5})_{1-x}Co_2$ and studied thermal expansion behavior. With tuning Gd concentration, ultra-low thermal expansion is realized in wide temperature intervals. The observed CTEs are even better than the well-known ZTE Invar alloys $Fe_{0.65}Ni_{0.35}$ (α_l ~1.5 × $10^{-6}K^{-1}$, 193-373 K) [1]. Detailed studies reveal that the introduction of Gd regulates the magnetovolume effect and the magnetostructural transition by mainly adjusting the c-axis in the rhombohedral FIM structure. The origin can be ascribed to the balance between the magnetostriction confined on c-axis and the normally anharmonic lattice vibration, as well as the suppression of lattice distortion by Gd doping.

$Gd_x(Ho_{0.5}Dy_{0.5})_{1-x}Co_2$(x=0, 0.1, 0.3, 0.5) compounds were prepared by arc-melting technique followed by annealing at 900°C for one month, and then quenched in liquid nitrogen. The crystal structure and thermal expansion behaviors were characterized by high resolution x-ray diffraction (XRD) using Cu-Kα target, which is equipped with a low-temperature chamber providing variable temperature within 5-300 K. The representative refined patterns are given in supplementary materials (see Fig. S1). Magnetization measurements were performed by using SQUID-VSM.

According to the general RCo_2 compounds, $Gd_x(Ho_{0.5}Dy_{0.5})_{1-x}Co_2$ exhibit FIM rhombohedral structure (space group: R-3m) below T_C, where Gd, Dy and Ho atoms randomly occupy Wycko-position 6c(0, 0, z) site, while Co_1 and Co_2 occupy two distinct sites of 3b(0, 0, 0.5) and 3b(0.5, 0, 0), respectively (Fig. 1a). The magnetic moments of R atoms (Gd, Dy and Ho) and Co are antiparallel along the c-axis in the rhombohedral structure. With increasing temperature, the compounds transform into PM cubic structure (space group: F-3m), where Gd, Dy and Ho atoms occupy 8a(0.125, 0.125, 0.125) site, while the Co atoms have one site 16d(0.5, 0.5, 0.5) (Fig. 1b).

Fig. 1c, d show the XRD patterns of samples x=0, 0.5, respectively, at selected temperatures from 5 to 300 K. The cubic phase and the corresponding index are marked by red while those for the rhombohedral phase by green. The (311) and (222) peaks of cubic phase corresponds to the (105^-), (201^-) and (006), (202) of rhombohedral phase, respectively. For x=0, the (311)/(105^-, 201^-), (222)/(006, 202) peaks obviously shift to higher 2θ, particularly around T_C~107K, with the transformation from rhombohedral FIM to cubic PM phase. This result indicates the occurrence of lattice contraction on heating. While for x=0.5, all the peaks including the (311)/(105^-, 201^-), (222)/(006, 202) remain nearly fixed independent of temperature even around T_C~274 K, implying that ultra-low thermal expansion prevails in the entire temperature range from 5K to 280K.

For details, the lattice volume and parameters refined based on the variable temperature XRD patterns are shown in Fig. 1e and Fig. 1f, respectively. The lattice volume monotonically increases with increasing the Gd content, since the Gd atomic radius is larger than Ho and Dy. From Fig. 1e, it can be seen that the specimen x=0 shows a step jump of lattice volume on cooling with ΔV/V~ -0.4% around T_C~107K, and the equivalent linear CTE can be as much as α_l ~ -3.6 × 10^{-5} K^{-1} in a narrow temperature interval ΔT~35K from 75K to 110K. With increasing Gd doping, the lattice distortion across phase transition can be suppressed, and the NTE around the T_C gradually flattens out. For x=0.3 and 0.5, the linear CTE around T_C reduces to be α_l ~ -3.4 × 10^{-6} K^{-1}(140K to 230K, ΔT~90K) and α_l ~ -1.5 × 10^{-6} K^{-1}(220K to 280K, ΔT~60K) in the extended temperature intervals, while the volume change is neglectable small, i.e. ΔV/V~ -0.1% and -0.03%, respectively. Moreover, below T_C, ultra-low thermal expansion appears in the broad interval for x=0.3 and 0.5 with CTE coefficients α_l ~ -9.9 × 10^{-7} K^{-1}(5K to 140K, ΔT~135K) and +1.3 × 10^{-6} K^{-1}(5K to 220K, ΔT~215K), respectively. The absolute values of these CTEs are both smaller than the well-known ZTE Invar alloy $Fe_{0.65}Ni_{0.35}$ (α_l ~1.5 × $10^{-6}K^{-1}$, 193-373 K, ΔT~180K) [1] while the operation temperature intervals can be much wider. The origin can be ascribed to the balance between the negative contribution of spontaneous magnetostriction and the conventional positive expansion of anharmonic lattice vibration. In $Gd_x(Ho_{0.5}Dy_{0.5})_{1-x}Co_2$, the magnetic moments of R and the antiparallel Co both align c-axis in the rhombohedral FIM structure (see Fig. 1a). So, it can be prompt to think that the negative contribution of spontaneous magnetostriction should mainly confine on the c-axis. Such speculation is well verified by the experimental observations. By taking x=0.5 as an example, the c-axis shows negative expansion in the temperature region below T_C while the a-axis displays totally positive expansion in contrast (Fig. 1f). The combined actions lead to the ultra-low thermal expansion in the broad temperature interval where the role of general lattice vibration has been naturally included. Moreover, since the Gd doping suppresses the lattice distortion around T_C (Fig. 1f), ultra-low thermal expansion is detected in the phase transition region for x=0.5 with α_l ~ -1.5 × 10^{-6} K^{-1}(220K to 280K, ΔT~60K). This is to say, for x=0.5, the absolute values of CTEs in the two intervals below and around T_C(5-280K, Fig. 1e) are better than or nearly the same as the performance of $Fe_{0.65}Ni_{0.35}$(α_l ~1.5 × $10^{-6}K^{-1}$, 193-373K, ΔT~180K) [1]. The ultra-low thermal expansion in such a broadened temperature interval is beneficial to practical applications. A rough estimation by linear fitting indicates that the average CTE for x=0.5 can be as low as α_l ~ +6.9 × $10^{-7}K^{-1}$ through the broad operation interval ΔT~275K(5~280K, top of Fig. 1e).

Fig. 1g summarizes the linear change of lattice, Δl/l, for specimens x=0, 0.3, and 0.5 deduced from Fig. 1e. The evolution of Δl/l with Gd doping is clearly manifested. In PM region without magnetic ordering, the positive expansion is totally determined by the conventional anharmonic lattice vibration. The $Gd_x(Ho_{0.5}Dy_{0.5})_{1-x}Co_2$ with different Gd doping show nearly the same CTE above T_C, noting that the V vs. T curve shows the same slope (Fig. 1e) and the Δl/l coincides with each other (Fig. 1g). This result indicates that the different Gd doping has little effect on the general anharmonic vibrations of atoms. In contrast, in the FIM region and phase transition region, $Gd_x(Ho_{0.5}Dy_{0.5})_{1-x}Co_2$ show distinct thermal expansion with varying Gd concentration, where the regulation effect of the introduced Gd on magnetic moments and hence atomic environments plays a dominated role.

To quantitatively characterize the effect of magnetism on lattice anomalies, magnetic measurements were performed and spontaneous magnetostriction behavior were analyzed. Fig. 2a demonstrates the temperature dependence of zero-field-cooled (ZFC) heating and field-cooling (FC) magnetization (M-T curve) under 0.05T for $Gd_x(Ho_{0.5}Dy_{0.5})_{1-x}Co_2$(x=0, 0.3, 0.5). As the Gd doping rises from x=0 to 0.5, T_C increases from 107 to 274K, while the thermal hysteresis remains almost zero. One can note that the magnetic transition temperature is nearly consistent with the

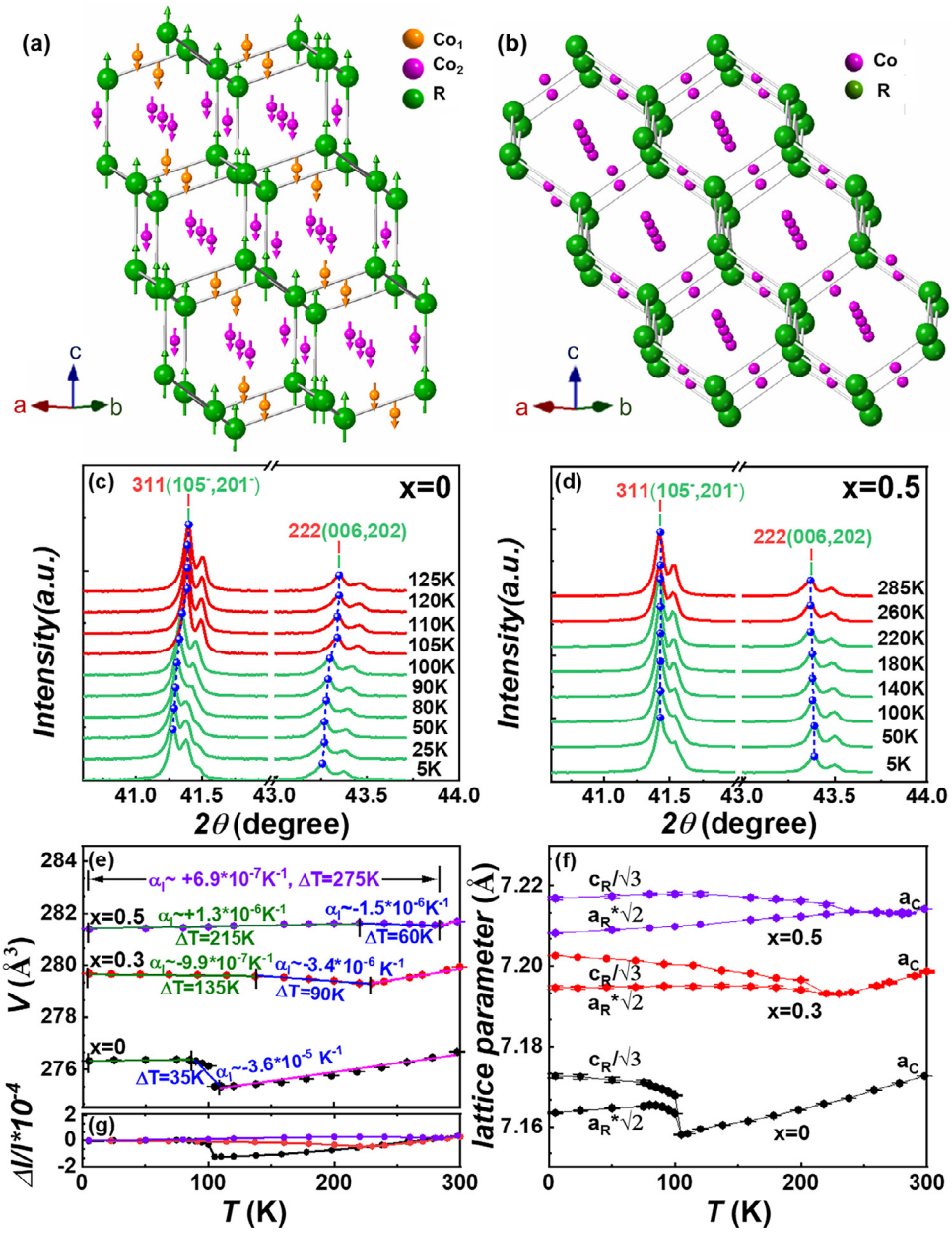

Fig. 1. The sketches of (a) rhombohedral FIM and (b) cubic PM structure of $Gd_x(Dy_{0.5}Ho_{0.5})_{1-x}Co_2$ compounds. Arrows indicate the directions of magnetic moments. The variable temperature XRD patterns around the cubic (311) and (222) peaks of $Gd_x(Ho_{0.5}Dy_{0.5})_{1-x}Co_2$ for (c) x=0 and (d) x=0.5, where the blue balls marked on the peaks' top and the lines guide eyes. Temperature dependence of (e) the lattice volume and (f) the lattice parameters for x=0, 0.3, 0.5, where the linear thermal coefficients α_l and the corresponding operation intervals ΔT are marked. (g) The comparison of linear change of lattice $\Delta l/l$ for x=0, 0.3, 0.5.

starting temperature of NTE (Fig. 1e), indicating that the magnetic behavior is closely related to the abnormal thermal expansion. Inset of Fig. 2a presents the M-T curves measured under 5T, from which the temperature dependence of molecular magnetic moment can be roughly deduced (Fig. 2b). One can find that the 5K magnetic moment reduces with increasing Gd content, which can be mainly ascribed to the magnetic dilution effect, noting that the moments of Gd ion ($7.94\mu_B$) is naturally smaller than either Ho ($10.6\mu_B$) or Dy ($10.6\mu_B$).

For the correlation between the ultra-low thermal expansion and magnetic behavior, spontaneous volume magnetostriction ω_s was used to quantitatively describe the contribution of magnetovolume effect to the abnormal thermal expansion. Fig. 3a, b show the decomposed thermal expansion characteristics for samples x=0.3 and 0.5, respectively. The ω_s in Fig. 3 is obtained by $\omega_s=\omega_{exp}-\omega_{nm}$, where $\omega_{exp}=\Delta V/V$ is the lattice volume change refined from XRD, and ω_{nm} is the one contributed from the normally anharmonic lattice vibration, which is calculated according to the Debye-Grüneisen relationship, [34] $\omega_{nm}=\gamma\frac{C_V k}{V_m}$, where γ and k are Grüneisen parameter and isothermal compressibility ($k=-(1/V)(dV/dP)_T$), $C_V=3N_0k_B$ and V_m are isochoric specific heat and molar volume, respectively. For the same specimen, the ω_{nm} in FIM region is nearly the same as that in PM region considering the same γ.

Fig. 3c shows the square of molecular magnetic moment (M^2) as a function of temperature (M^2-T curve) for x= 0.3, 0.5, while Fig. 3d correspondingly displays the ω_s accorded from Fig. 3a and 3b. By comparing Fig. 3c and 3d, the close relation between M^2

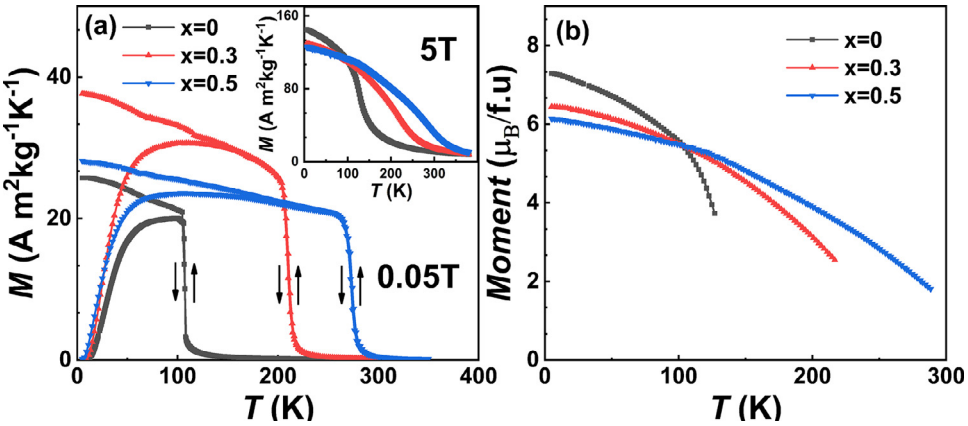

Fig. 2. (a) Temperature dependence of ZFC-FC magnetization for $Gd_x(Ho_{0.5}Dy_{0.5})_{1-x}Co_2$ (x=0, 0.3, 0.5) under 0.05T on heating and cooling. Inset shows the M-T curves measured under 5T for the corresponding samples. (b) Temperature dependence of molecular magnetic moment in FIM region deduced from the inset of (a).

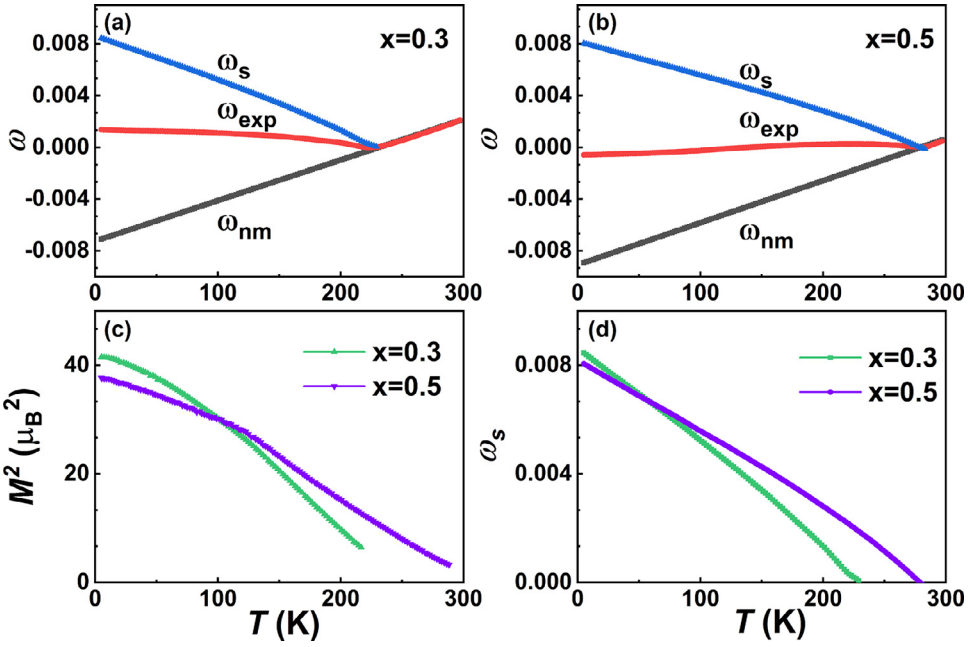

Fig. 3. Decomposed thermal expansion characteristics of $Gd_x(Ho_{0.5}Dy_{0.5})_{1-x}Co_2$ for (a) x=0.3 and (b) x=0.5. Temperature dependence of (c) the square of molecular magnetic moment (M^2) and (d) spontaneous volume magnetostriction ω_s for x=0.3, 0.5.

and ω_s can be identified. Generally, the ω_s(T) can be described by following equation, [35,36]

$$\omega_s(T) = kCM(T)^2 \quad (1)$$

where k is the isothermal compressibility, C is the magnetovolume coupling constant, and M(T) is the molecular magnetic moment. This means that the magnetovolume effect is totally determined by the evolution of magnetic moment with temperature, which can be adjusted by introducing substitution of Ho, Dy by Gd in $Gd_x(Ho_{0.5}Dy_{0.5})_{1-x}Co_2$. The fitting of $\omega_s(T) \sim M(T)^2$ is performed, which obeys the equation (1), see details in supplementary materials. As shown in Fig. 3c, the M^2 at 5K for x=0.3 is higher than that of x=0.5. But the M^2 for x=0.5 falls slower than x=0.3 with increasing temperature because x=0.5 has a higher T_C. Consistent with the trend of M^2-T curve, the ω_s of x=0.3 at 5K is also higher than that of x=0.5, while the ω_s of x=0.5 also falls slower than x=0.3 in the corresponding temperature region (Fig. 3d). Note that the ω_{nm} from the normally anharmonic lattice vibration is nearly independent of the Gd content (Fig. 1e, g). Therefore, the combined effect from the magnetostriction and the normally anharmonic lattice vibration results in the ultra-low thermal expansion but with different signs for x=0.3 and x=0.5. The CTE sign is negative for x=0.3, i.e. $\alpha_l \sim -9.9 \times 10^{-7}$ K^{-1}(5K to 140K, ΔT~135K), while positive CTE for x=0.5, i.e. $+1.3 \times 10^{-6}$ K^{-1}(5K to 220K, ΔT~215K) in a much wider temperature interval. The magnetic moments of R ions align c-axis in the rhombohedral FIM structure (Fig. 1a). From Fig. 1f, one can find that the c-axis length shows negative thermal expansion for both x=0.3 and x=0.5 while the trend with temperature is also the same as the M^2-T and ω_s -T (Fig. 3c, d), that is, the c-axis length of x=0.5 falls slower than x=0.3 with increasing temperature. This result further indicates that the arrangements of R ions in $Gd_x(Ho_{0.5}Dy_{0.5})_{1-x}Co_2$ dominates the magnetostriction process.

Moreover, we also studied MCE of $Gd_x(Ho_{0.5}Dy_{0.5})_{1-x}Co_2$ by magnetic measurements. Fig. 4a and 4b show the magnetization isotherms (M-H curve) for x=0 and x=0.5, respectively. For x=0 with sharp volume change during the magnetostructural transition (Fig. 1e), the M-H curves present "S" shape at temperatures above but close to T_C, indicating the metamagnetic transition driven by magnetic field. But what's fascinating is that no hysteresis ap-

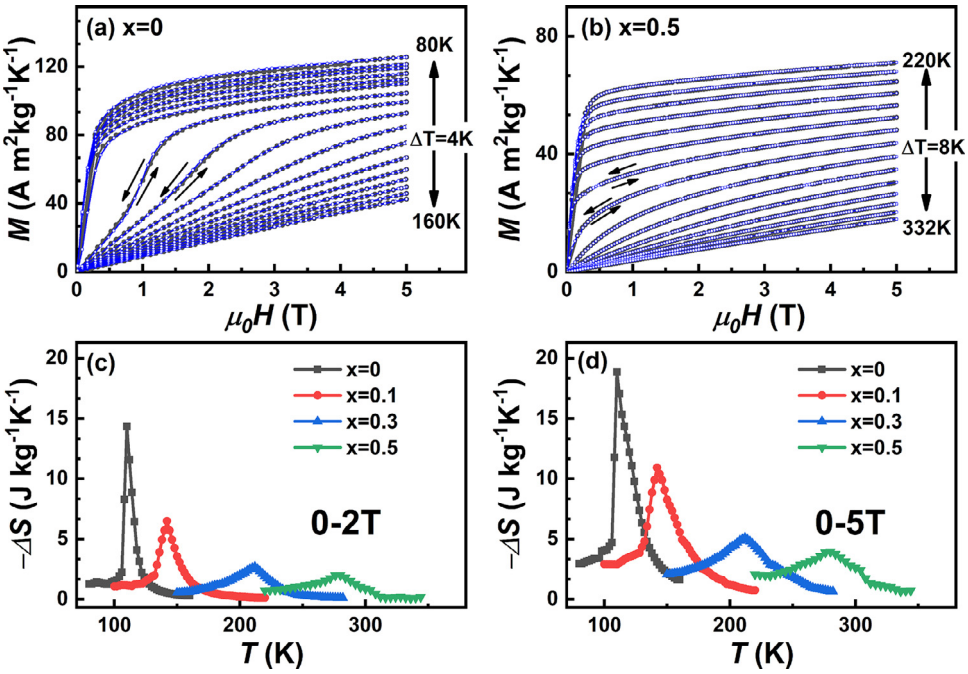

Fig. 4. Magnetization isotherms of $Gd_x(Ho_{0.5}Dy_{0.5})_{1-x}Co_2$ compounds on field ascending and descending for (a) x=0 and (b) x=0.5. Entropy change ΔS under (c) 0-2T and (d) 0-5T magnetic field change for the samples with various Gd contents, x=0, 0.1, 0.3, 0.5.

pears in the magnetic field cycle (Fig. 4a), which is an appreciate characteristic from view of optimizing efficiency. The exact physical origin for the non-hysteretic first-order phase transition is unclear at the moment, which requires further studies. The entropy change was calculated using Maxwell relation $\Delta S = \int_0^H (\frac{\partial M}{\partial T})_H dH$, which is the total entropy change contributed from both spin and lattice [37,38]. For x=0, the -ΔS reaches ~14.3 and ~18.8 J $kg^{-1}K^{-1}$ at 110K for 0-2T and 0-5T, respectively. These ΔS magnitudes are considerable large compared to others available in the low-temperature region [39]. With increasing Gd doping, the volume change around T_C becomes less sharp and eventually approaches zero for x=0.5 (Fig. 1e). It means the contribution from lattice to the ΔS is getting smaller and even becomes zero. Moreover, the molecular magnetic moment also reduces notably because of the magnetic dilution effect. The combined effect leads to a rapid reduction of ΔS while the peak shifts to high temperature as the Gd doping rises (see Fig. 4c, d). For x=0.1, the -ΔS is ~10.9 J $kg^{-1}K^{-1}$(0-5T) at 142K, while it quickly reduces to ~3.9 J $kg^{-1}K^{-1}$(0-5T) at 280K for x=0.5.

In summary, ultra-low thermal expansion is achieved in $Gd_x(Dy_{0.5}Ho_{0.5})_{1-x}Co_2$ compounds. At low Gd contents x=0, 0.1, the materials show considerable MCE owing to the significant lattice contribution during magnetostructural transition. While for x=0.3, 0.5, ultra-low thermal expansion is demonstrated. The origin can be ascribed to the balance between magnetovolume effect and general anharmonic lattice vibration in FIM region, where the arrangements of R ions along c-axis in the rhombohedral FIM phase play a dominated role in regulating the magnetostriction process. Moreover, ultra-low thermal expansion also occurs in the phase transition region around T_C for x=0.5 owing to the suppression of lattice distortion by Gd doping. As a result, the CTEs α_l ~+1.3 × $10^{-6}K^{-1}$(5-220K), -1.5 × $10^{-6}K^{-1}$(220-280K) are even better in a significantly broadened temperature interval compared to the ZTE Invar alloy $Fe_{0.65}Ni_{0.35}$ (α_l ~1.5 × $10^{-6}K^{-1}$, 193-373K, ΔT~180K), and a rough estimation by linear fitting indicates that the average CTE can be as low as α_l ~ +6.9 × $10^{-7}K^{-1}$ through ΔT~275K(5~280K). This work not only broadens the categories of exploring anomalous thermal expansion in the area of MCE materials, but also highlights the advantageous ways to generate ultra-low thermal expansion.

Declaration of Competing Interest

The authors declare that they have no known competing financial interests or personal relationships that could have appeared to influence the work reported in this paper.

Acknowledgments

This work was supported by the National Key Research and Development Program of China [Grant Nos. 2017YFB0702702, 2019YFA0704904, 2018YFA0305704, 2017YFA0206300, 2017YFA0303601, and 2016YFB0700903], the National Natural Science Foundation of China [Grant Nos. U1832219, 51531008, 51771223, 51590880, 51971240, 11674378, 11934016, 11921004], and the Key Program and Strategic Priority Research Program (B) of the Chinese Academy of Sciences.

Supplementary materials

Supplementary material associated with this article can be found, in the online version, at doi:10.1016/j.scriptamat.2020.04.043.

References

[1] C. Guillaume, C. Seances, CR. Acad. Sci 125 (1897) 18.
[2] T. Mary, J. Evans, T. Vogt, A. Sleight, Science 272 (5258) (1996) 90–92.
[3] X.G. Zheng, H. Kubozono, H. Yamada, K. Kato, Y. Ishiwata, C.N. Xu, Nat. Nanotechnol 3 (12) (2008) 724–726.
[4] J. Chen, X.R. Xing, C. Sun, P.H. Hu, L.H. Li, J. Am. Chem. Soc 130 (4) (2008) 1144–1145.
[5] S. Iikubo, K. Kodama, K. Takenaka, H. Takagi, M. Takigawa, S. Shamoto, Phys. Rev. Lett 101 (20) (2008) 205901.
[6] X.G. Guo, J.C. Lin, P. Tong, M. Wang, Y. Wu, C. Yang, B. Song, S. Lin, W.H. Song, Y.P. Sun, Appl. Phys. Lett 107 (20) (2015) 202406.
[7] Y. Sun, C. Wang, Q.Z. Huang, Y.F. Guo, L.H. Chu, M. Arai, K. Yamaura, Inorg. Chem 51 (13) (2012) 7232–7236.

[8] K. Takenaka, H. Takagi, Appl. Phys. Lett 94 (13) (2009) 131904.
[9] R. Huang, Y. Liu, W. Fan, J. Tan, F. Xiao, L. Qian, L. Li, J. Am. Chem. Soc. 135 (31) (2013) 11469–11472.
[10] Y.Y. Zhao, F.X. Hu, L.F. Bao, J. Wang, H. Wu, Q.Z. Huang, R.R. Wu, Y. Liu, F.R. Shen, H. Kuang, J. Am. Chem. Soc. 137 (5) (2015) 1746–1749.
[11] K. Takenaka, Y. Okamoto, T. Shinoda, N. Katayama, Y. Sakai, Nat. Commun 8 (2017) 14102.
[12] S.E. Tallentire, F. Child, I. Fall, L. Vella-Zarb, I.R. Evans, M.G. Tucker, D.A. Keen, C. Wilson, J.S. Evans, J. Am. Chem. Soc 135 (34) (2013) 12849–12856.
[13] A.E. Phillips, G.J. Halder, K.W. Chapman, A.L. Goodwin, C.J. Kepert, J. Am. Chem. Soc 132 (1) (2010) 10–11.
[14] H. Xu, P.J. Heaney, D.M. Yates, R.B. Von Dreele, M.A. Bourke, J. Mater. Res 14 (7) (1999) 3138–3151.
[15] L. Hu, J. Chen, L.L. Fan, Y. Ren, Y.C. Rong, Z. Pan, J.X. Deng, R.B. Yu, X.R. Xing, J. Am. Chem. Soc 136 (39) (2014) 13566–13569.
[16] S. Margadonna, K. Prassides, A.N. Fitch, J. Am. Chem. Soc 126 (47) (2004) 15390–15391.
[17] X.Y. Song, Z.H. Sun, Q.Z. Huang, M. Rettenmayr, X.M. Liu, M. Seyring, G.N. Li, G.H. Rao, F.X. Yin, Adv. Mater 23 (40) (2011) 4690–4694.
[18] Y.Z. Song, J. Chen, X.Z. Liu, C.W. Wang, J. Zhang, H. Liu, H. Zhu, L. Hu, K. Lin, S.T. Zhang, X.R. Xing, J. Am. Chem. Soc 140 (2) (2018) 602–605.
[19] V.K. Pecharsky, K.A. Gschneidner Jr, Phys. Rev. Lett 78 (4) (1997) 4.
[20] F.X. Hu, B.G. Shen, J.R. Sun, Z.H. Cheng, G.H. Rao, X.X. Zhang, Appl. Phys. Lett 78 (23) (2001) 3675–3677.
[21] S. Fujieda, A. Fujita, K. Fukamichi, Appl. Phys. Lett 81 (7) (2002) 1276–1278.
[22] H. Wada, Y. Tanabe, Appl. Phys. Lett 79 (20) (2001) 3302–3304.
[23] E. Brück, J. Kamarad, V. Sechovsky, Z. Arnold, O. Tegus, F.R. de Boer, J. Magn. Magn. Mater 310 (2) (2007) e1008–e1009.
[24] N.T. Trung, V. Biharie, L. Zhang, L. Caron, K.H.J. Buschow, E. Brück, Appl. Phys. Lett 96 (16) (2010) 162507.
[25] H. Wada, S. Tomekawa, M. Shiga, Cryogenics 39 (11) (1999) 915–919.
[26] N.A. de Oliveira, P.J. von Ranke, M.V. Tovar Costa, A. Troper, Phys. Rev. B 66 (9) (2002) 094402.
[27] N.K. Singh, K.G. Suresh, A.K. Nigam, S.K. Malik, A.A. Coelho, S. Gama, J. Magn. Magn. Mater 317 (1-2) (2007) 68–79.
[28] I.P. Zhuravleva, G.E. Grechnev, A.S. Panfilov, A.A. Lyogenkaya, Low Temp. Phys 43 (5) (2017) 597–601.
[29] S.L. Driver, J. Herrero-Albillos, C.M. Bonilla, F. Bartolome, L.M. Garcia, C.J. Howard, M.A. Carpenter, J Phys Condens Matter 26 (5) (2014) 056001.
[30] P.J. von Ranke, N.A. de Oliveira, J. Appl. Phys 83 (11) (1998) 6967–6968.
[31] K. Morrison, A. Dupas, Y. Mudryk, V.K. Pecharsky, K.A. Gschneidner, A.D. Caplin, L.F. Cohen, Phys. Rev. B 87 (13) (2013) 134421.
[32] R. Lizárraga, Phys. Rev. B 94 (17) (2016) 174201.
[33] Z.W. Ouyang, F.W. Wang, Q. Hang, W.F. Liu, G.Y. Liu, J.W. Lynn, J.K. Liang, G.H. Rao, J. Alloys Compd 390 (1-2) (2005) 21–25.
[34] P.F.F. Sayetat, M. Kessler, J. Appl. Crystallogr 31 (1998) 7.
[35] T. Moriya, K. Usami, Solid State Commun 34 (2) (1980) 95–99.
[36] A. Fujita, K. Fukamichi, J.T. Wang, Y. Kawazoe, Phys. Rev. B 68 (10) (2003) 104431.
[37] P.J.v. Ranke, N.A. de Oliveira, C. Mello, A.M.G. Carvalho, S. Gama, Phys. Rev. B 71 (5) (2005) 054410.
[38] K.A. Gschneidner Jr., V.K. Pecharsky, A.O. Tsokol, Rep. Prog. Phys 68 (6) (2005) 1479–1539.
[39] V. Franco, J.S. Blázquez, J.J. Ipus, J.Y. Law, L.M. Moreno-Ramírez, A. Conde, Prog. Mater Sci 93 (2018) 112–232.